Title no. 104-M17

Compressive Behavior of Ultra-High-Performance Fiber-Reinforced Concrete

by Benjamin A. Graybeal

An experimental program was conducted to determine the uniaxial compressive behaviors of an ultra-high performance fiber-reinforced concrete (UHPFRC). Cylinders were tested in compression and the results were analyzed to determine the strength, modulus of elasticity, strain capacity, and overall stress-strain behaviors of both untreated and steam-treated UHPFRC. The results show that this concrete exhibits exceptional compressive strength and enhanced stiffness. Predictor equations for the strength gain with time and the modulus of elasticity as a function of compression strength are presented. The linearity of the stress-strain response of this concrete is discussed and an equation for the ascending branch of the compressive stress-strain behavior is established.

Keywords: compressive strength; fiber-reinforced concrete; modulus of elasticity.

INTRODUCTION

Ultra-high performance fiber-reinforced concrete (UHPFRC) is a new class of concrete that has been developed in recent years. When compared with high performance concrete (HPC), UHPFRC exhibits superior properties in terms of compressive behaviors, tensile behaviors, and durability. A research program was initiated to characterize many of the behaviors relevant to the use of UHPFRC in the highway bridge industry (Graybeal 2006). This paper discusses the specific results that are relevant to the compressive behavior of UHPFRC.

Compression testing of cylinders is a frequently used quality control method for structural concrete, therefore, engineers often attempt to relate other characteristics of concrete's behavior to this parameter. Countless researchers have worked to develop relationships between the compressive strength of concrete and other stress- and strain-based properties. Of particular interest herein are relationships between concrete compressive strength and the uniaxial strain the concrete experiences when subjected to compressive loads.

The empirical relationship between compressive strength and modulus of elasticity is one such relationship. Equation (1) provides one of the simplest and most widely used relationships for normal strength concrete (ACI Committee 318 2005)

$$E = 4730\sqrt{f'_c} \quad \text{in MPa} \qquad (1)$$
$$E = 57{,}000\sqrt{f'_c} \quad \text{in psi}$$

where the square root of the compressive strength is related to the modulus of elasticity through a linear multiplier. Other more sophisticated relationships may include a term for the density of the concrete, the compressive strength raised to different fractional power, or the inclusion of a constant term (Popovics 1998; Neville 1996). Other relationships considered in this study include the equations from ACI 363R (ACI Committee 363 1992), AASHTO-LRFD (2007), CEB-FIB Model Code (1990, 1993, 1995), Norwegian Standard 3473 (1992), Acito et al. (1999), Kakizaki et al. (1992), and Ma et al. (2004), the last two of which were developed from ultra-high-strength concrete test results. Equations (2) and (3) present the ACI 363R and Ma et al. equations, respectively. Note that the ACI 363R equation was proposed for concretes up to 83 MPa (12 ksi), while the Ma et al. equation was derived from experimental results on UHPFRC containing no coarse aggregates. These two equations most closely predict the results observed in this study.

$$E = 3320\sqrt{f'_c} + 6900 \text{ in MPa} \qquad (2)$$
$$E = 40{,}000\sqrt{f'_c} + 1{,}000{,}000 \text{ in psi}$$

$$E = 19{,}000\sqrt[3]{\frac{f_c'}{10}} \text{ in MPa} \qquad (3)$$
$$E = 525{,}000\sqrt[3]{\frac{f_c'}{10}} \text{ in psi}$$

One of the potentially most useful concrete parameter relationships relates the stress-strain behavior of the material to the compressive strength and the modulus of elasticity. Unfortunately, the compressive stress-strain responses of different concretes exhibit significant variation because, among other things, concrete is a heterogeneous material without standardized mixture designs. Many researchers have presented empirically-based numerical approximations for the ascending branch or the ascending and descending branches of the compressive stress-strain behavior of particular concretes. This body of research, however, has resulted in minimal consensus on any one equation's formulation or applicability to concrete in general (Neville 1996; Popovics 1998; Carreira and Chu 1985). Furthermore, there are currently no prevalent relationships that were derived from or are considered relevant to the uniaxial compressive stress-strain behavior of this particular UHPFRC. Given this lack of published relationships, the research discussed herein focuses on determining straightforward relationships between the compressive strength, the modulus of elasticity, and the uniaxial compressive stress-strain behavior of this new type of concrete.

ACI Materials Journal, V. 104, No. 2, March-April 2007.
MS No. M-2006-052.R1 received June 9, 2006, and reviewed under Institute publication policies. Pertinent discussion including authors' closure, if any, will be published in the January-February 2008 *ACI Materials Journal* if the discussion is received by October 1, 2007.

Benjamin A. Graybeal *is a Research Structural Engineer for the Federal Highway Administration at the Turner-Fairbank Highway Research Center, McLean, Va. His research interests include concrete material characterization, experimental evaluation of highway bridge structures, and nondestructive evaluation techniques.*

Table 1—Typical UHPFRC composition

Material	Amount, kg/m^3 (lb/yd^3)	Percent by weight
Portland cement	710 (1200)	28.5
Fine sand	1020 (1720)	40.8
Silica fume	230 (390)	9.3
Ground quartz	210 (355)	8.4
High-range water-reducing admixture	31 (51.8)	1.2
Accelerator	30 (50.5)	1.2
Steel fibers	156 (263)	6.2
Water	110 (184)	4.4

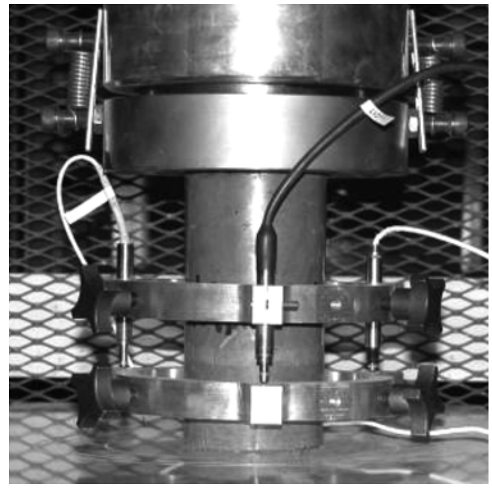

Fig. 1—Axial displacement measuring apparatus.

RESEARCH SIGNIFICANCE

Recent advances in concrete technology have allowed for the development of concretes that exhibit significantly enhanced compressive strengths and stiffnesses. Practical use of these concretes requires knowledge of the basic compressive behaviors of the concrete as well as knowledge of the interrelationship between uniaxial stress and strain. The research discussed herein focuses on determining these basic behaviors and defining the interrelationships.

EXPERIMENTAL INVESTIGATION

This research focused on characterizing the compressive behaviors of the one UHPFRC currently commercially available in the U.S. This high cement, high silica fume content concrete has an extremely low water-cement ratio (*w*/*c*) (less than 0.20) and uses the new generation of high-range water-reducing admixtures (polycarboxylate base) to achieve an acceptable workability. This concrete contains no coarse aggregate and is internally reinforced by 13 mm (0.5 in.) long straight steel fibers included at 2% by volume. The approximate mixture composition used throughout this research is presented in Table 1. Note that the effect of the fiber reinforcement on the compressive properties of this concrete was not studied, as this type of concrete is nearly always steel fiber reinforced when used in a structural application.

The results presented in this paper are based on compression tests of 76 mm (3 in.) diameter, approximately 150 mm (6 in.) long cylinders loaded in axial compression. The concrete was mixed in a 56 L (2 ft^3) laboratory pan mixer then placed into molds. The molds were filled while on a vibrating table, following standard procedures for fiber-reinforced concrete. Approximately 1 day after casting, the cylinders were demolded.

Two curing regimes were applied to the cylinders after demolding. Some of the cylinders were steam treated, wherein the cylinders were subjected to 48 hours of curing in a steam environment (90 °C, 95% humidity). After this treatment, these cylinders were stored in a standard laboratory environment (22 °C, variable humidity ranging from 30 to 50%) until testing. The remainder of the cylinders were stored in the laboratory environment from demolding until testing. These curing regimes were designed to mimic the range of potential conditions that could be experienced by match-cast cylinders associated with large precast structural elements composed of this concrete. The steam-treated regime is normally recommended for this concrete, while the untreated regime is the minimum curing condition that could be implemented, assuming that the resulting limited behaviors were acceptable.

The cylinder compression tests were completed primarily according to ASTM C 39. The only noteworthy exception to the test method was the loading rate; it was set at 1 MPa/second (150 psi/second) due to the high compressive strength of this concrete. The capture of the strain behavior of the UHPFRC cylinders was completed according to ASTM C 469. For these tests, an axial displacement measuring device was attached to the cylinders to capture the axial strain. This device, which consisted of two rings mounted on the cylinder and a trio of LVDTs to measure the distance change between the rings, is shown in Fig. 1. The apparatus was attached below the center of each specimen due to test setup constraints; however, as the lower attachment point was at least 25 mm (1 in.) above the bottom of the specimen, it is not anticipated that end constraint effects had any impact on the test results. Tests completed with this device were run continuously from load initiation through failure without stopping the test to remove the device. Uniform load application on each cylinder was guaranteed by monitoring the three axial displacement gauges on the cylinder throughout the initial stages of each test. Calculation of the modulus of elasticity for each cylinder was based on the LVDT displacement readings captured at loads between 10 and 30% of the peak load carried by the cylinder.

TEST RESULTS AND ANALYSIS

Compressive strength, modulus of elasticity, and strain at peak strength

The compressive strength results presented in this paper were collected as part of a larger study of the mechanical and durability properties of UHPFRC. The compressive strength of 76 mm (3 in.) diameter cylinders was the control parameter for all batches of concrete cast in this study. In total, the results from 138 cylinders cast within 22 batches were averaged to determine that the 28-day, steam-treated compressive strength was 193 MPa (28.0 ksi) with a 14 MPa (2.0 ksi) standard deviation. The results from 88 cylinders cast within 13 batches were averaged to determine that the 28-day, untreated compressive strength was 126 MPa (18.3 ksi) with a 14 MPa (2.0 ksi) standard deviation.

The modulus of elasticity results are based on select cylinders not included in the compressive strength results. The testing

Table 2—Strength, modulus of elasticity, and strain at peak stress results at various ages after casting

Test age, days	Compressive strength, MPa (ksi): No. of cylinders	Average	Standard deviation*	Modulus of elasticity, GPa (ksi): No. of cylinders	Average	Standard deviation*	Strain at peak stress: No. of cylinders	Average	Standard deviation*
Steam-treated									
1.3	5	26.9 (3.9)	2.7 (0.36)	5	19.4 (2820)	1.9 (278)	5	0.0068	0.0008
5	5	185 (26.8)	6.2 (0.92)	5	52.4 (7600)	0.8 (109)	4	0.0041	0.0005
15	6	193 (28.0)	5.5 (0.75)	6	52.5 (7620)	1.1 (162)	4	0.0040	0.0003
30	6	200 (28.9)	6.9 (0.97)	6	51.4 (7460)	1.2 (167)	4	0.0046	0.0003
55	6	194 (28.1)	8.3 (1.20)	6	52.5 (7610)	0.7 (99)	4	0.0039	0.0003
Untreated									
1.0	3	15.2 (2.2)	1.4 (0.20)	3	10.5 (1520)	2.1 (312)	3	0.0094	0.0019
2.0	2	64.8 (9.4)	0.7 (0.10)	2	28.3 (4100)	0.6 (76)	3	0.0050	0.0005
3	2	73.1 (10.6)	0.7 (0.08)	2	36.0 (5220)	0.3 (43)	3	0.0039	0.0003
7	3	88.9 (12.9)	0.7 (0.09)	3	39.0 (5660)	0.8 (111)	3	0.0036	0.0008
9	2	101 (14.7)	4.1 (0.59)	2	37.6 (5450)	0.8 (112)	3	0.0034	0.0016
14	6	110 (16.0)	4.1 (0.61)	6	41.2 (5970)	1.2 (172)	6	0.0037	0.0006
28	6	119 (17.2)	3.4 (0.53)	6	41.9 (6070)	1.1 (164)	4	0.0034	0.0001
57	6	125 (18.1)	4.8 (0.69)	6	42.0 (6090)	1.0 (146)	3	0.0036	0.0002

*In groups that only include two or three cylinders, standard deviation is provided solely as indication of dispersion.

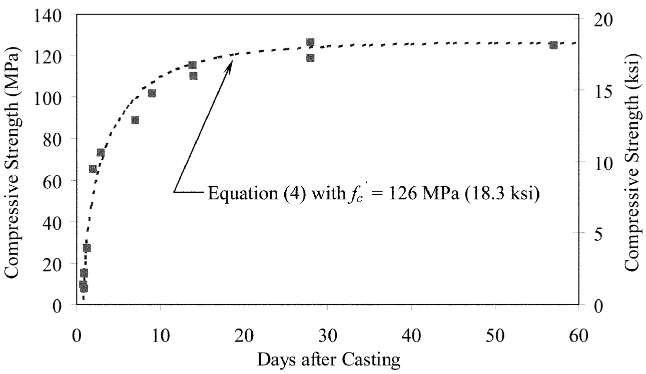

Fig. 2—Compressive strength gain of untreated UHPFRC as function of time after casting.

of 30 cylinders from five different batches resulted in a steam-treated UHPFRC modulus of elasticity of 52.7 GPa (7650 ksi) with a 1.5 GPa (220 ksi) standard deviation at 28 days. The untreated UHPFRC was found to have a 28-day modulus of elasticity of 42.7 GPa (6200 ksi) with a 1.5 GPa (220 ksi) standard deviation based on 18 samples from four batches. Because continuous axial displacement data was collected throughout the entire compressive loading of the cylinders, the axial strain at peak compressive strength was also determined. For the steam-treated cylinders, this value is 0.0041 with a standard deviation of 0.0004. The untreated regime at 28 days exhibited a strain at peak strength of 0.0035 with a standard deviation of 0.0002. Note that these results, which are based on a larger body of tests, are very similar to the results discussed in the next section and presented in Table 2 for similar specimens tested at various ages after casting.

Compressive properties as function of time

Additional testing of cylinders of various ages from within individual batches provides an indication of the change in compressive properties over time. Table 2 presents the results from two batches, one for each curing regime. The number of tests included in each result is listed in the table. These results indicate that the compressive strength of this concrete is effectively stabilized at the conclusion of a 48-hour steam treatment. In contrast, the untreated concrete tends to continue to gain compressive strength for at least 8 weeks after casting. Other testing completed within this research program indicates that delaying the steam treatment of cylinders up to 8 months after casting can still increase the compressive strength of the cylinders by approximately 25% as compared with their untreated value (Graybeal 2006).

The results shown in Table 2, along with ASTM C 403 penetration resistance testing for set time determination, indicate that this UHPFRC does not have any appreciable compressive strength until many hours after casting. For this particular mixture design, initial set was found to occur approximately 15 hours after mixing with final set occurring approximately 2 hours later. Set time, however, has been observed to vary widely for these types of concretes depending on the high-range water-reducing admixture, the specific cementitious materials, and on whether an accelerator is used. For this particular concrete, a similar mixture design that did not include an accelerator resulted in initial set occurring up to 36 hours after mixing.

Once setting had occurred, the concrete rapidly gained strength such that 70 MPa (10 ksi) of strength was achieved 2 days later. Note, however, that the workability of this UHPFRC changes soon after casting such that, even though initial set has not occurred, further working of the concrete is not possible.

Figure 2 presents a compilation of the compressive strength data for the untreated cylinders tested between 1 and 56 days. A regression analysis was completed to fit a function to the data presented in the figure. The delayed then rapid early age strength gain behavior of this UHPFRC results in a somewhat complex approximating function. The Weibull Cumulative function, provided as Eq. (4) and plotted in Fig. 2, accurately describes the untreated UHPFRC strength gain behavior for any time after 0.9 days following casting. This equation includes the time in days after casting t, the untreated UHPFRC 28-day compressive strength in MPa f_c', and the untreated UHPFRC compressive strength at time t in MPa $f_{c,t}'$. The initial and final set times of this UHPFRC were found to vary depending on the age of the premix and the environmental conditions surrounding the unset concrete, thus this equation may not be applicable to other concretes exhibiting different setting behaviors.

$$f'_{c,t} = f_c'\left[1 - \exp\left(-\left(\frac{t-0.9}{3}\right)^{0.6}\right)\right] \quad (4)$$

Full compression stress-strain response data was also collected for each of the cylinder sets presented in Table 2. These results clearly illustrate the change in the behavior of UHPFRC as the curing of the concrete progresses. Figure 3 shows axial compressive stress-strain responses for untreated UHPFRC cylinders at various ages after casting. In particular, note that as the compressive strength increases, the pre-peak nonlinearity and the post-peak strain capacity both decrease. Comparison of additional responses associated with steam-treated cylinders indicates that, regardless of the age of the cylinder, after the steam treatment is applied, the basic shape of the ascending branch of the compressive stress-strain response remains unchanged.

Relationship between modulus of elasticity and compressive strength

As discussed previously, various empirical relationships exist to relate the compressive strength of concrete to its modulus of elasticity. A comparison of some of the more prevalent published relationships to the data obtained in this study indicates that some relationships are more applicable than others.

The data for this analysis included results from both steam-treated and untreated curing regime cylinders of any age that exhibited at least 25 MPa (3.6 ksi) of compressive strength. Additionally, data from two other curing regimes (one in which the temperature of the steam treatment was decreased and one in which the steam treatment was delayed for 2 weeks) were also included. In total, results from 97 samples were used to populate the range of compressive strengths from 25 to 195 MPa (3.6 to 28.3 ksi). Note that sets of similar cylinders were grouped, averaged, and weighted for the curve fitting analysis and in the plotting of the results.

The data, which was the basis for this analysis, along with the modulus results for strengths below 25 MPa (3.6 ksi), are shown Fig. 4. This figure also graphically presents the ACI 363R and Ma et al. equations (Eq. (2) and (3)). These equations exhibited the best performance of any previously published relationship studied with R-squared values of 0.957 and 0.881, respectively. It should be observed, however, that more experimental results were available in the higher portion of the strength range, thus these equations' large overestimation of the modulus of elasticity at lower strengths is not borne out by lower R-squared values.

An alternative modulus of elasticity predictor equation was developed to more accurately predict the full range of compressive strengths that this concrete exhibits. It was determined that the form of Eq. (1) accurately represented the shape of the UHPFRC relationship and only a modification of the scalar factor was required. The result of this analysis is Eq. (5) that exhibits an R-squared value of 0.967. This relationship is also shown in Fig. 4. As is shown in the figure, the adjustment of the scalar factor in Eq. (1) to the value shown in Eq. (5) allows for a simple equation that reflects that behavior of this UHPFRC at strengths above 25 MPa (3.6 ksi).

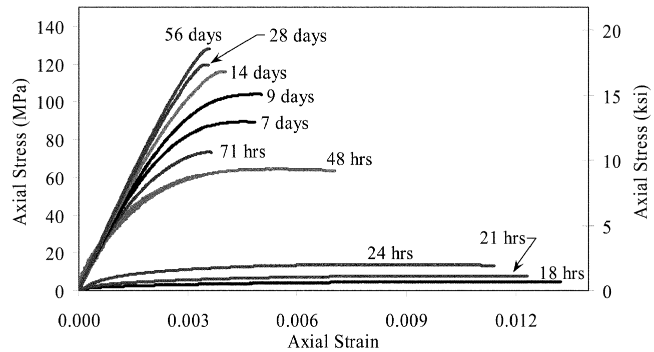

Fig. 3—Selected stress-strain responses for untreated UHPFRC.

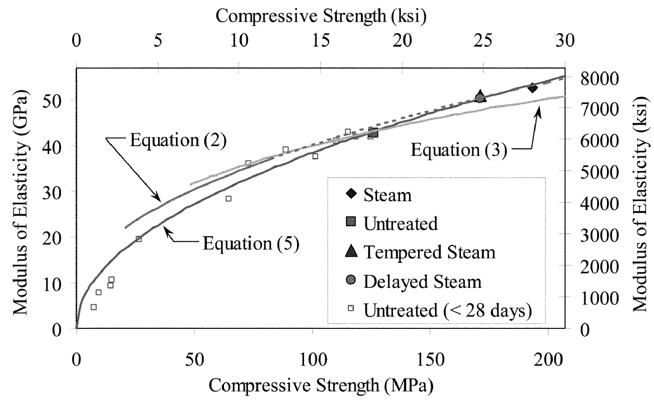

Fig. 4—Modulus of elasticity as function of compressive strength.

$$E = 3840\sqrt{f_c'} \text{ in MPa} \qquad E = 46{,}200\sqrt{f_c'} \text{ in psi} \quad (5)$$

Linearity of compressive stress-strain response

It is normally assumed that concrete begins to develop internal microcracking and exhibit an associated reduction in stiffness as compressive stresses are increased. The degradation varies depending on the composition of the concrete. The linearity of the compressive stress-strain response of this UHPFRC was investigated to determine the stress level at which significant nonlinearity is apparent.

One traditional method for determining the linearity of a concrete stress-strain response is to determine the secant modulus for the strain at peak strength. The secant modulus E_0 is then compared to the ASTM C 469 modulus of elasticity to determine the linearity of the compression behavior. For reference, the ratio of these values is normally approximately 3.5 for normalweight 7 MPa (1 ksi) compressive strength concrete and approximately 1.25 for 70 MPa (10 ksi) compressive strength concrete (Popovics 1998). For this UHPFRC, the ratio of the moduli values illustrates how the compressive behavior changes with curing procedure and with time. At 1 day ($f_c' \approx 7$ MPa [1 ksi]) after casting, the ratio for this untreated UHPFRC ranges from 5 to 7. By 3 days ($f_c' \approx 70$ MPa [10 ksi]), it is under 2. The ratio for this untreated UHPFRC ($f_c' \approx 126$ MPa [18.3 ksi]) tends to stabilize at approximately 1.2 after 28 days. For stream treated cylinders ($f_c' \approx 193$ MPa [28.0 ksi]), a ratio of approximately 1.1 is observed after the steam curing is complete.

Table 3—Compressive stress-strain response linearity at various ages after casting

Test age, days	Compressive strength, MPa (ksi)	Strain at peak stress	E/E_0	No. of cylinders	Linearity, 1%		Linearity, 3%		Linearity, 5%	
					Strain	Stress, MPa (ksi)	Stain	Stress, MPa (ksi)	Strain	Stress, MPa (ksi)
Steam-treated										
1.3	26.9 (3.9)	0.0068	4.90	5	0.000340	6.5 (0.94)	0.000420	7.6 (1.1)	0.000470	8.3 (1.2)
5	185 (26.8)	0.0041	1.16	5	0.001730	90 (13.0)	0.002790	141 (20.5)	0.003400	169 (24.5)
15	193 (28.0)	0.0040	1.09	6	0.001830	95 (13.8)	0.002890	147 (21.3)	0.003440	172 (24.9)
30	200 (28.9)	0.0046	1.18	5	0.001930	99 (14.4)	0.002960	149 (21.6)	0.003620	177 (25.7)
55	194 (28.1)	0.0039	1.06	6	0.001870	97 (14.1)	0.002960	151 (21.9)	0.003700	184 (26.7)
Untreated										
1.0	15.2 (2.2)	0.0094	6.49	2	0.000330	3.0 (0.43)	0.000380	3.8 (0.55)	0.000410	4.1 (0.59)
2.0	64.8 (9.4)	0.0050	2.20	0	—	—	—	—	—	—
3	73.1 (10.6)	0.0039	1.90	2	0.000590	21 (3.0)	0.000740	26 (3.7)	0.000870	30 (4.3)
7	88.9 (12.9)	0.0036	1.59	3	0.000680	26 (3.8)	0.000930	35 (5.1)	0.001140	42 (6.1)
9	101 (14.7)	0.0034	1.26	2	0.000920	34 (5.0)	0.001250	46 (6.6)	0.001520	54 (7.9)
14	110 (16.0)	0.0037	1.39	6	0.000860	34 (5.0)	0.001200	48 (6.9)	0.001490	58 (8.4)
28	119 (17.2)	0.0034	1.21	6	0.001040	43 (6.2)	0.001530	62 (9.0)	0.001930	77 (11.1)
57	125 (18.1)	0.0036	1.20	6	0.001180	49 (7.1)	0.001760	72 (10.4)	0.002220	88 (12.8)

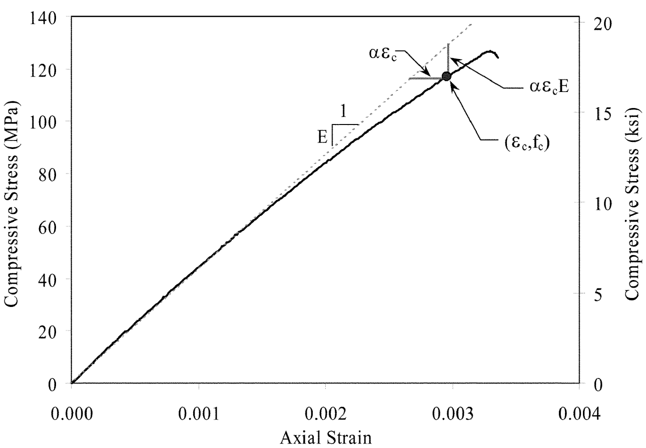

Fig. 5—Compressive stress-strain behavior compared with linear elastic response.

The linearity as defined by the secant modulus does not provide any indication of the stress level where nonlinear behaviors become evident. Further analysis was completed, focusing on the specific stress levels where 1, 3, and 5% stress deviations from linear elastic behavior occurred. This analysis technique is shown graphically in Fig. 5, where the actual stress (f_c) and strain (ε_c) values are related to the linear elastic behavior through the coefficient α that defines the percent stress decrease from linear elastic behavior.

The linearity results—in terms of the stress at which the stress will have dropped some percentage from the linear elastic expected value—are presented in Table 3. The results from the 5% drop show that this steam-treated UHPFRC exhibits nearly linear behavior to high stress levels. Cylinders that underwent steam treatment reach between 80 and 90% of their compressive strength before diverging 5% from linear elastic behavior. The untreated cylinders seem to be asymptotically approaching the same type of response by 8 weeks after casting, having reached 70% of their compressive strength before diverging 5% from the linear elastic behavior.

Compressive stress-strain behavior

As discussed previously, a consensus regarding potential numerical relationships for the stress-strain behavior of concrete does not currently exist. This can be partially attributed to the inherent variability that exists between different concretes and partially attributed to the difficulties inherent in the process of experimentally capturing these behaviors. From an experimental standpoint, gathering consistent, accurate stress and strain data from the full range of compressive behavior response is very difficult. This fact is primarily due to the increasingly nonlinear behaviors that concrete tends to exhibit as the strain at the compressive strength is reached and surpassed. Even if the descending branch of the behavior is ignored, as the compressive strength is approached, the observed straining behavior of the concrete becomes very dependent on the experimental loading and strain measurement techniques employed.

The preceding discussion leads to the conclusion that any experimentally obtained stress-strain data points from earlier in the concrete response are likely more accurate than strain values from later in the concrete response. The concrete compressive strength f_c' and the concrete modulus of elasticity E can both be considered to be relatively accurate based on experimental results. The concrete strain at the compressive strength and the associated secant modulus, however, are both based on strain measurements that are more difficult to accurately capture and thus are less accurately known. This fact points to a weakness of many models of concrete compressive stress-strain behavior as they are based on an accurate knowledge of the compressive strain at the peak strength. Even if the stress-strain response was captured accurately in an initial research program that defined a particular relationship, this relationship will be less useful to practitioners or other researchers as subsequent use will be dependent on accurate determination of strains near peak stress.

Therefore, an analytical technique was implemented in this research program wherein the stress-strain relationship is defined by an equation based primarily on the compressive strength and the modulus of elasticity. The stress-strain relationship is defined in Eq. (6), which shows that the stress and strain are related by the modulus of elasticity and a reduction factor α, which defines the decrease in the actual stress from the linear elastic stress. This is the same concept that was used to define linearity in the previous section of this paper.

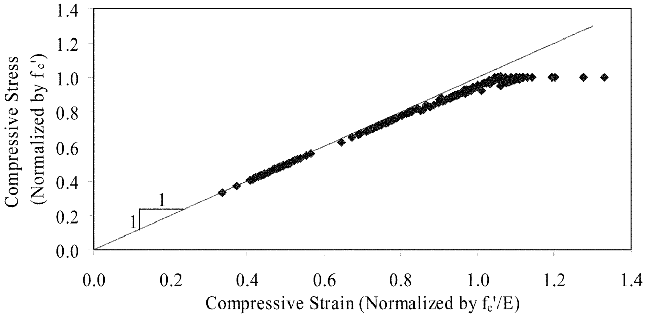

Fig. 6—Normalized compressive stress-strain results for steam-treated UHPFRC.

$$f_c = \varepsilon_c E(1 - \alpha) \quad (6)$$

Just as in the previous linearity discussion, the present analysis included specific intermediate benchmarks in the behavior that were defined and collected for each cylinder tested. These points included the strain where α equaled 1, 3, 5, and possibly 10% (if reached). One additional point was defined for each specimen wherein either the peak stress and corresponding strain had been reached or the final reliable ascending branch data point had been reached due to impending discontinuity in the stress-strain behavior. Thus, a compressive strength, a modulus of elasticity, and four or five pairs of stress-strain points defining the ascending branch characterized the behavior of each cylinder. As such, the effect of inaccuracies inherent in strain measurements near the peak strength are reduced by these measurements contributing to less than 25% of the data points used to define the shape of the ascending branch of the curve.

The stress-strain pairs for each specimen were normalized based on the compressive strength and modulus of elasticity. Note that, although the compressive stress normalization is based on the experimentally obtained compressive strength, the strain normalization is based on the theoretical linear elastic strain at the compressive strength. This particular normalization technique also reduces the overall inaccuracy within the analysis by avoiding the use of a variable that is difficult to capture accurately, namely the average strain at the compressive strength.

This analysis was completed for both the steam-treated UHPFRC and for the 28-day behavior of the untreated UHPFRC. Figure 6 displays the benchmarks defined for the collection of steam-treated UHPFRC cylinders, along with the average linear elastic behavior defined for this curing regime, on a normalized stress-strain plot. This figure clearly shows the general shape that an ascending branch approximation must match to accurately represent the compressive behavior. This view of the data, however, does not allow for easy differentiation between potential fitting curves. A more accurate representation of the overall behavior can be obtained by focusing on the deviation of the actual behavior of the concrete compared with the theoretical linear elastic response. Figure 7 presents the same benchmarks in terms of the decrease from the linear elastic response, again compared with the normalized strain. This presentation highlights the behaviors that must be captured in the model.

Approximation curves were fit to the data sets for both curing regimes. An exponential function, again normalized on the linear elastic strain at the compressive strength, was found to fit the data moderately well. This is shown below as

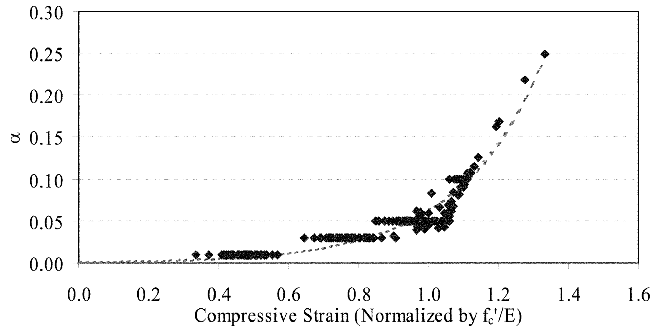

Fig. 7—Deviation from linear elastic compressive behavior for steam-treated UHPFRC.

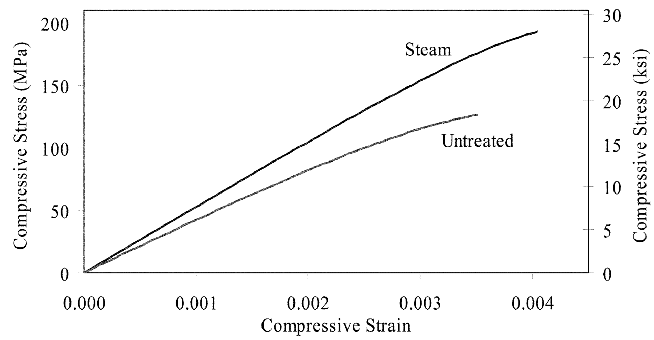

Fig. 8—Compressive stress-strain response approximations.

Eq. (7). The two fitting parameters in the equation, *a* and *b*, are 0.001 and 0.24, respectively, for the steam-treated regime. For the untreated regime, the parameter values are 0.011 and 0.44. Figure 7 shows the accuracy with which this curve fits the experimentally captured results.

$$\alpha = ae^{\frac{\varepsilon_c E}{bf_c'}} - a \quad (7)$$

The analysis discussed previously results in an equation for the ascending branch of the compressive stress-strain response of this concrete. The ascending branch curves for the steam-treated and untreated UHPFRC, defined via the insertion of α from Eq. (7) into Eq. (6), are shown in Fig. 8. Based on these equations and the experimentally determined 28-day compressive strength and modulus of elasticity, the strain at peak compressive strength is predicted to be 0.0041 for the steam-treated regime and 0.0037 for the untreated regime.

Although the constants *a* and *b* were developed herein for this UHPFRC, the basic methodology can be used to calibrate the relationship for other concretes. The experimental testing required for this calibration is no different than that required by other researchers who base their stress-strain relationships on the value of the strain at the peak stress. In this formulation, however, the accuracy of the result should be increased due to the reasons discussed previously.

CONCLUSIONS

Based on the results of this experimental investigation of the compressive behavior of an ultra-high performance concrete, the following conclusions are drawn:

1. This UHPFRC exhibits an exceptionally high compressive strength and a significantly higher modulus of elasticity as

compared to normal and high performance concrete; however, the strain at peak stress is only slightly higher than would normally be expected for concrete;

2. The strength gain of this UHPFRC is initially restrained, but once initiated, it occurs very rapidly with over 70 MPa (10 ksi) of compressive capacity developing within 2 days of setting without any supplemental curing treatment being applied. Steam treatment causes the strength to dramatically increase and to stabilize at approximately 193 MPa (28 ksi);

3. The modulus of elasticity of this UHPFRC, regardless of the curing treatment, is predictable within the compressive strength range of 25 to 193 MPa (3.6 to 28 ksi). The ACI 363R equation predicts the behavior moderately well, especially at higher strengths, while a modified version of the ACI 318 equation was determined to provide the most accurate representation overall;

4. The compressive stress-strain response of the steam-treated concrete is within 5% of linear elastic at 80% of its compressive strength. For the untreated concrete at 8 weeks after casting, the limiting value is 70% of its compressive strength; and

5. The ascending branch of the compressive stress-strain behavior of this UHPFRC has been defined in terms of its deviation from linear elastic behavior. Constants for the steam-treated and untreated regimes have been provided. Constants for alternate concretes could be developed via the methodology presented.

ACKNOWLEDGMENTS

The research that is the subject of this paper was funded by the Federal Highway Administration. The author gratefully acknowledges this support. The publication of this article does not necessarily indicate approval or endorsement of the findings, opinions, conclusions, or recommendations either inferred or specifically expressed herein by the Federal Highway Administration or the U.S. Government.

NOTATION

E = modulus of elasticity
f_c = compressive stress in concrete corresponding to ε_c
f'_c = compressive strength of concrete
$f'_{c,t}$ = compressive strength of concrete at time t
t = time, days after casting
α = percent stress decrease from linear elastic predicted stress
ε_c = compressive strain in concrete corresponding to f_c

REFERENCES

AASHTO-LRFD, 2007, "Bridge Design Specifications," American Association of State Highway and Transportation Officials, Washington, D.C., 1485 pp.

ACI Committee 318, 2005, "Building Code Requirements for Structural Concrete (ACI 315-05) and Commentary (318R-05)," American Concrete Institute, Farmington Hills, Mich., 430 pp.

ACI Committee 363, 1992, "Report on High-Strength Concrete (ACI 363R-92)," American Concrete Institute, Farmington Hills, Mich., 55 pp.

Acito, M.; Guerrini, G.; and Migliacci, A., 1999, "On the Correlation Between the Modulus of Elasticity and the Compressive Strength in VHSC," *Proceedings of the 5th International Symposium on the Utilization of High Strength/High Performance Concrete*, Sandefjord, Norway, June, pp. 947-955.

Carreira, D. J., and Chu, K.-H., 1985, "Stress-Strain Relationship for Plain Concrete in Compression," ACI Journal, *Proceedings* V. 82, No. 6, Nov.-Dec., pp. 797-804.

Comité Européen du Beton, 1990, "High Strength Concrete, State of the Art Report," *CEB Bulletin* 197, Aug., Lausanne, Switzerland, 61 pp.

Comité Européen du Beton, 1993, "CEB-FIP Model Code 1990," *Design Code*, Lausanne, Switzerland, 437 pp.

Comité Européen du Beton, 1995, "High Performance Concrete, Recommended Extensions to the Model Code 90, Research Needs," *CEB Bulletin* 228, July, Lausanne, Switzerland, 60 pp.

Graybeal, B. A., 2006, "Material Property Characterization of Ultra-High Performance Concrete," *Report* No. FHWA-HRT-06-103, Federal Highway Administration, Washington, D.C., Aug., 186 pp.

Kakizaki, M., 1992, "Effect of Mixing Method on Mechanical Properties and Pore Structure of Ultra-High Strength Concrete," *Katri Report* No. 90, Kajima Corporation, Tokyo, Japan, 19 pp.

Ma, J.; Dehn, F.; Tue, N. V.; Orgass, M.; and Schmidt, D., 2004, "Comparative Investigations on Ultra-High Performance Concrete with and without Coarse Aggregates," *Proceedings of the International Symposium on Ultra-High Performance Concrete*, Kassel, Germany, Sept., pp. 205-212.

Neville, A. M., 1996, *Properties of Concrete*, 4th Edition, John Wiley & Sons, Inc., New York, 844 pp.

Norwegian Council for Building Standardization, 1992, "Design of Concrete Structures," *Norwegian Standard* NS 3473, Oslo, Norway, 78 pp.

Popovics, S., 1998, *Strength and Related Properties of Concrete*, John Wiley & Sons, Inc., New York, 522 pp.